

Synthesis, Structure, Antibacterial Activity, and Hirshfeld Surface Analysis of Complex [Co(4-ampy)₄(NCS)₂] \cdot CO₂

Linggar Agil Savitri¹, Faaza'izzahaq Setta Putra¹, Sutandyo Dwija Laksana²,
Dewi Mariyam¹, and I Wayan Dasna^{1,2*}

¹Department of Chemistry, Faculty of Mathematics and Natural Sciences, Universitas Negeri Malang, Jl. Semarang No. 5, Malang 65145, Indonesia

²Center of Advanced Material for Renewable Energy, Universitas Negeri Malang, Jl. Semarang No. 5, Malang 65145, Indonesia

* Corresponding author:

email: idasna@um.ac.id

Received: November 10, 2023

Accepted: March 14, 2024

DOI: 10.22146/ijc.90585

Abstract: The [Co(4-ampy)₄(NCS)₂] \cdot CO₂ complex compound was successfully synthesized using the reflux method from the reaction between CoCl₂ \cdot 6H₂O, 4-aminopyridine, and KSCN in methanol solvent for 6 h at 64 °C. The synthesized compound is a dark purple cube-shaped crystal with a melting point of 209 °C. FTIR test showed the presence of isothiocyanate anion at C=N stretching vibration wavenumber 1633 cm⁻¹, C-N vibration on amine group belonging to 4-aminopyridine ligand at 1217 cm⁻¹, and C=N vibration of pyridine aromatic group at 1334 cm⁻¹. Single crystal X-ray diffraction data refinement results show the complex compound has octahedral geometry in a cubic lattice with space group $P\bar{n}3n$ with lattice parameters $a = b = c = 16.426(3)$ Å and $\alpha = \beta = \gamma = 90^\circ$. According to the crystal data, there was one molecule of CO₂ in the crystal packing of the complex. Hirshfeld surface analysis showed the major interaction contributions from C \cdots H/H \cdots C, H \cdots H, S \cdots H/H \cdots S, and O \cdots H/H \cdots O. The antibacterial activity test results showed that the activity of the synthesized complex was more active against *Staphylococcus aureus* but less effective against *Escherichia coli*.

Keywords: cobalt complex; 4-aminopyridine ligand; thiocyanate anion; Hirshfeld surface

■ INTRODUCTION

Complex compounds have become an essential topic in coordination chemistry in the last decade [1]. The diversity of coordination patterns, crystal structures, biological activities, and magnetic properties are studies that attract researchers [2]. From the variety of complexes synthesized, transition metals are used as central atoms because they have empty valence shell orbitals that can accept electron pairs from ligands. Complexes of cobalt(II), nickel(II), copper(II), and zinc(II) ions have been synthesized and tested for their benefits as antimicrobial [3], antibacterial [4], anticancer [5], antifungal [6] and cosmetic industries [7].

Cobalt is a transition metal used to synthesize complex compounds that have the potential as antibacterial and antiviral [8] The antibacterial activity of

Co(II) metal is equivalent to complexes of V(IV), Cu(II), Zn(II), and Pd(II) metals [9]. Co(II) based complex compounds such as [Co(2-ampy)₂(SCN)₂] (2-ampy = 2-aminopyridine, SCN = thiocyanate) were shown to have antibacterial properties against *Staphylococcus aureus* and *Salmonella typhi* [10-11]. Cobalt has the ability to form complexes with a variety of biomolecules, making them applicable to a diverse range of biological uses. Complexes with cobalt metal can form varied geometries: planar quadrilateral, octahedral, tetrahedral, and octahedral [12]. The characteristics of transition metals can be adjusted by coordinating them with various ligands. This adjustment encompasses stabilizing different oxidation states and altering the solvophilicity, electrophilic, and nucleophilic traits of the metal ion. In the coordination chemistry field, the properties of metal ions are not only modified, but also

those of the ligands themselves. Utilizing different ligands allows for the adjustment of cobalt compound properties to closely match those of cellular processes, due to similar ligand exchange rates [13].

Complex compounds containing pyridine ligands and their derivatives show antibacterial properties against Gram-positive and Gram-negative bacteria [14-18]. Pyridine derivative ligands such as x-aminopyridine (x = 2, 3, 4) have a large molecular size to expand the accessible area against the bacterial surface, and the amino group can interact with the bacterial cell wall to change its structure to penetrate the bacterial lipid layer. Several complex compounds with pyridine and aminopyridine ligands, such as Mn(2-ampy)₂(dca)₂ [19], [Cu(py)₂(SCN)₂]_n [3], [Co(dca)₂(2-ampy)₂] [10-11], Zn(2-ampy)₂(NCS)₂ [20-21], and Ni(2-ampy)₂(dca)₂ [22], (py = pyridine, dca = dicyanamide) [22-23] showed antibacterial activity against *Escherichia coli*, *S. aureus*, and other bacteria. However, the antibacterial activity value is still below chloramphenicol.

The synthesized Co(II) complex contains 2-ampy, with an amino group in the ortho position. Aminopyridine derivatives such as meta- and para-aminopyridine are interestingly studied for their antibacterial properties because they have more open amino groups than 2-ampy. The interaction of the amino group with the bacterial surface can be more potent. The effect of the octahedral geometry of the complex compound on its antibacterial properties needs to be studied considering the [Co(2-ampy)₂(SCN)₂] [10-11] complex in previous studies. This complex has a tetrahedral geometry, where apart from the type of aminopyridine derivative, the amount of bound aminopyridine can also affect the antibacterial properties of the complex.

This study reports the synthesis and characterization of complex compounds using cobalt(II) salt, 4-ampy, and thiocyanate anion. Thiocyanate (SCN⁻) or isothiocyanate (NCS⁻) ions can act as bidentate ligands because they have two donor atoms of N and S. Complex compounds with thiocyanate ligands also show good antibacterial properties, so in this study, thiocyanate anions were used as anion ligands. *In vitro* antibacterial activity of the resulting complexes was tested against *S.*

aureus and *E. coli*. Hirshfeld surface analysis will also be carried out to determine the interactions in the crystal.

■ EXPERIMENTAL SECTION

Materials

The materials used included CoCl₂·6H₂O (Emsure ACS; p.a.; 98.00%), KSCN (Aldrich Chemistry; p.a.; 98.00%), 4-aminopyridine (Emsure ACS; p.a.; 98.00%), methanol (Merck; p.a.; 98.00%), and distilled water. The materials were directly used without additional treatment.

Instrumentation

The tools used in the synthesis of complex compounds are glassware, filter paper, stirrer, magnet, set of reflux apparatus, and analytical balance. The characterization of the complex was done using a melting point apparatus (Fisher-John Scientific Melting Point Apparatus), FTIR instrumentations with KBr Pellet test technique (Shimadzu IR Prestige 21), and single-crystal XRD (Bruker, D8 Quest Diffractometer, λ: Mo).

Procedure

Synthesis of [Co(4-ampy)₄(NCS)₂]·CO₂ complex compound

The synthesis method refers to the research of Munadhiroh et al. [10] and Mariyam et al. [21]. The Co(II) complex that was successfully synthesized by the reflux method was Co(2-ampy)₂(NCS)₂ with 13 d of evaporation [10]. The synthesis begins with weighing the compound 4-ampy (0.3764 g, 4 mmol), and dissolved in 5 mL of methanol. The 4-ampy was refluxed for 30 min at 64 °C. Then, a solution of CoCl₂·6H₂O (0.2379 g, 1 mmol) in 5 mL of methanol was refluxed for 3.5 h. Then, KSCN solution (0.1944 g, 2 mmol) was added and refluxed for 2 h. The synthesis was then filtered, and the resulting filtrate was put into a glass beaker to evaporate slowly. Needle-shaped crystals and dark purple cubes were obtained after evaporation for 18 d. Melting point: 209 °C; Electrical conductivity.: 158.5 μS; FTIR (cm⁻¹): 3460 (m) ν_s(N-H); 3338 (m) ν(N-H); 1516 (s) ν(N-H); 1338 (m) ν(C-N); 2092 (s) ν(C≡N); 1633 (s) ν(C=N).

Characterization of $[\text{Co}(4\text{-ampy})_4(\text{NCS})_2]\cdot\text{CO}_2$ complexes

Melting point tests were carried out in temperatures of 30–300 °C with a temperature increase range of 10 °C/min. FTIR analysis was done in the 500–4000 cm^{-1} region. Crystallinity and structural analysis were also performed using a Bruker single crystal XRD device.

Antibacterial activity test

The antibacterial activity test used the Kirby Bauer disc diffusion method. Firstly, Muller-Hinton agar medium was prepared with procedures according to the manufacturer's commercial instructions against *E. coli* (ATCC 25922) and *S. aureus* (ATCC 25923) bacteria [19]. Then, specific bacterial colonies were suspended in 0.9% NaCl solution. Bacterial turbidity was tested according to 0.5 McFarland standard, equivalent to a bacterial concentration of 1.5×10^8 CFU/mL. Samples were tested by weighing the synthesized crystals, cobalt(II) chloride, 4-ampy, and KSCN, and chloramphenicol antibiotics dissolved in methanol solvent at a concentration of 1 mg/mL. Paper discs were sterilized with an autoclave and then dipped in the solution for 20 min. The discs were placed on agar media and incubated at 37 °C for 24 h, and then the diameter of the inhibition zone was measured and compared to the reactants and products formed.

Hirshfeld surface analysis

Using Crystal Explorer software, Hirshfeld surface analysis aims to calculate intermolecular interactions determined by Crystallographic Information File (CIF) data [24-25]. CIF is the refinement data from single crystal XRD.

RESULTS AND DISCUSSION

Synthesis and Physical Properties of Complex

The cobalt(II) salt and ligands were reacted directly

in CH_3OH as a solvent with the mol ratio $\text{Co(II)}:4\text{-NH}_2\text{py}:\text{KSCN}$ of 1:4:2. The results gave dark-purple crystals with cube-shaped (Fig. 1). The reaction of complex formation is presented in Fig. 2. The CO_2 trapped in the crystal system is captured directly from the air. Several previous studies have shown that some complexes are able to absorb CO_2 and carry out spontaneous fixation, such as zinc(II) tetraazacycloalkane and $[\text{Ni}(\text{N,N}\text{-Me}_2\text{en})_3](\text{ClO}_4)_2$ ($\text{N,N}\text{-Me}_2\text{en} = \text{N,N}$ -dimethylethylenediamine). Meanwhile, in this reaction, the complex was only able to capture CO_2 without a fixation reaction occurred.

The complex was air-stable and had sharp melting points at 209 °C. The melting point data of the complex was higher $[\text{Co}(\text{NCS})_2(2\text{-NH}_2\text{py})_2]$ [10]. This could be due to the amount of aminopyridine bound to Co is more significant, so the size of the complex was larger compared to $[\text{Co}(\text{NCS})_2(2\text{-NH}_2\text{py})_2]$. The complex solutions have been measured for their electrical conductivity in 1 mg/mL using methanol solvent and showed the result 158.5 μS . This result indicates that complex solutions were weak electrolytes [26].



Fig 1. Crystal of the complex

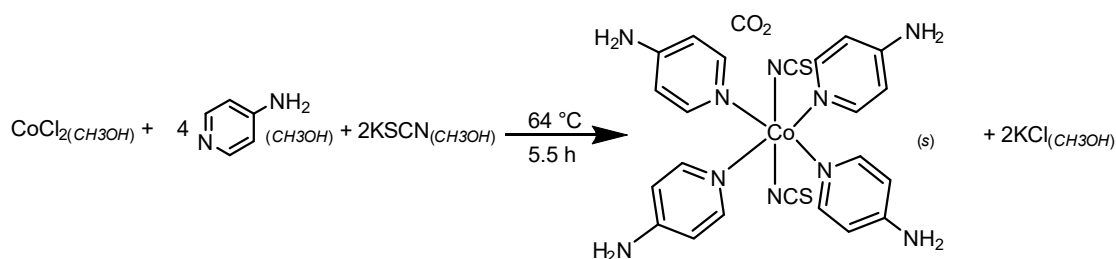


Fig 2. Reaction of complex formation

FTIR Analysis

The FTIR test was carried out to determine the functional groups that bind to central ion in complex compound. The test was carried out using a spectrophotometer in the wavenumber range of 4000–400 cm^{-1} (Fig. 3). The characteristics of the 4-ampy ligand are shown at wavenumbers of 3542, 3439, and 3303 cm^{-1} (Table 1) which are asymmetric and symmetric $\nu(\text{N-H})$ [20]. Asymmetric and symmetric $\nu(\text{N-H})$ bond vibrations of 4-ampy in complex appear at 3460, 3338, and 3209 cm^{-1} . The asymmetric and symmetric stretching vibrations of the $-\text{NH}_2$ group experienced a slight shift, indicating the formation of hydrogen bonds between the $-\text{NH}_2$ group and the thiocyanate ligand. The appearance of 3 stretching vibration bands of $-\text{NH}_2$ indicates a primary amine group [20-21]. The presence of the 4-ampy ligand is indicated by the N-H vibration of the amine group, which is also observed at a wavelength of 1583 cm^{-1} , which experiences a significant shift to 1516 cm^{-1} . In addition, the considerable shift of $\nu(\text{C-N})$ of aromatic ring from 1334 to 1338 cm^{-1} indicates the bond formation of the N donor atom of the pyridine ring [22-23].

The thiocyanate ion can bind through the S or N atoms, as observed in the FTIR spectrum. The vibration of $\text{C}\equiv\text{N}$ experienced a shift towards smaller wavenumbers, indicating that the thiocyanate ion binds through the N atom. In comparison, the peak of the S-C stretching vibration will shift to larger wavenumbers, indicating that the thiocyanate ion forms a bond through the S atom. The characteristic absorption band of the thiocyanate ion ligand is shown in the $\text{C}\equiv\text{N}$ vibration at a

wavelength of 2160 cm^{-1} , which shifts to 2092 cm^{-1} , and the $\text{C}=\text{N}$ vibration appearing at a wavelength of 2080 cm^{-1} shifts to a smaller wavelength, specifically at 2056 cm^{-1} . The observed shift in wavelength towards smaller values indicates the presence of terminal ligand coordination bonds on the thiocyanate ion through the N atom, which reinforces the XRD data.

Single Crystal XRD

The reaction of $\text{CoCl}_2 \cdot 6\text{H}_2\text{O}$ with 4-ampy and KSCN produced a high-quality single crystal of the complex compound $[\text{Co}(\text{4-ampy})_4(\text{NCS})_2] \cdot \text{CO}_2$. The single crystal was then analyzed for its structure using single-crystal XRD. The crystallographic data of the complex compound is shown in Table 2. The crystal structure refinement uses APEX4 software and the resulting structure is generated using Mercury 4.2.0 program shown in Fig. 4–6. Fig. 4 shows that the Co(II)

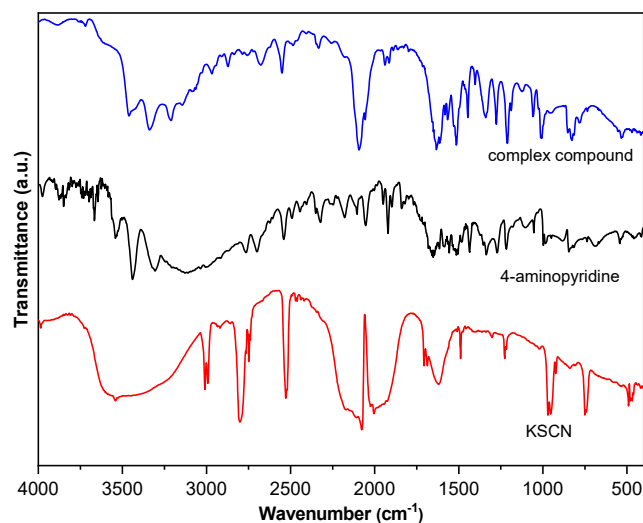


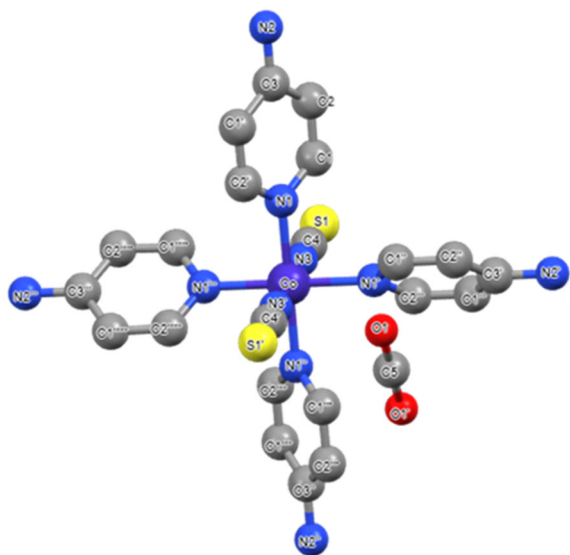
Fig 3. FTIR spectra of complex and its ligands

Table 1. Interpretation of FTIR spectra of complex and its ligands

Vibration	Wavenumber (cm^{-1})		
	4-aminopyridine	thiocyanate	$[\text{Co}(\text{4-ampy})_4(\text{NCS})_2] \cdot \text{CO}_2$
$\nu_s(\text{N-H})$	3542	-	3460
$\nu_{as}(\text{N-H})$	3439	-	3338
$\nu(\text{N-H})$	1583	-	1516
$\nu(\text{C-N})$	1334	-	1338
$\nu(\text{C-N})$	1217	-	1211
$\nu(\text{C}\equiv\text{N})$	-	2160	2092
$\nu(\text{C}=\text{N})$	-	2080	2056
$\nu(\text{C}=\text{N})$	-	1620	1633

Table 2. Crystallographic data of $[\text{Co}(\text{4-ampy})_4(\text{NCS})_2]\cdot\text{CO}_2$

Crystallographic data	$[\text{Co}(\text{4-ampy})_4(\text{NCS})_2]\cdot\text{CO}_2$
Chemical formula	$\text{C}_{70}\text{H}_{72}\text{Co}_3\text{N}_{30}\text{O}_8\text{S}_6$
M_r (g/mol)	1830.72
Crystal system	Cubic
Space group	$\text{P}\bar{3}\text{n}$
Temperature (K)	296
$a = b = c$ (Å)	16.426(3)
$\alpha = \beta = \gamma$ (°)	90
V (Å ³)	4432(2)
Z	2
Radiation type	Mo K α
μ (mm ⁻¹)	0.76
Crystal size (mm)	$0.3 \times 0.27 \times 0.21$
$T_{\text{min}}, T_{\text{max}}$	0.669, 0.746
No. of measured, independent and observed [$I > 2\sigma(I)$] reflections	13399, 872, 631
R_{int}	0.023
$\sin \theta/\lambda_{\text{max}}$ (Å ⁻¹)	0.651
$R[F^2 > 2\sigma(F^2)], wR(F^2), S$	0.049, 0.177, 1.04
No. of reflections	872
No. of parameters	50
$\Delta\rho_{\text{max}}, \Delta\rho_{\text{min}}$ (e Å ⁻³)	1.26, -0.55

**Fig 4.** The structure of $[\text{Co}(\text{4-ampy})_4(\text{NCS})_2]\cdot\text{CO}_2$ complex

center ion binds coordinately with six N atoms derived from four N atoms of the pyridine ring of the 4-ampy ligand and two N atoms of the isothiocyanate ligand, forming an octahedral geometry. Based on HSAB theory, N atoms, which are borderline bases, tend to be attracted to Co metal, which is also a borderline acid, compared to

S donor atoms, which are soft bases. The 4-ampy is a monodentate ligand, and the isothiocyanate is a terminal ligand because it only donates one donor atom.

The structure of the complex compound also shows the presence of CO_2 molecules that are free in the crystal lattice and not in a state bound to the molecules of complex compounds, as shown in Fig. 5. The CO_2 molecules can come from CO_2 in the air that comes into the complex during the heating process with reflux. Table 2 shows that the complex compound crystallizes in the cube crystal system, and the space group $\text{P}\bar{3}\text{n}$, where each lattice side length and angle is the exact value of $a = b = c = 16.426(3)$ Å and $\alpha = \beta = \gamma = 90^\circ$, respectively.

The asymmetric unit of the complex compound structure contains only a quarter of the molecule, even in the 4-ampy ligand, the pyridine ring also shows half of the whole ring. One crystal lattice contains two molecules of the complex compound $[\text{Co}(\text{4-ampy})_4(\text{NCS})_2]\cdot\text{CO}_2$. The absence of changes in the position of the molecular arrangement seen in the packing of the crystal lattice from the point of view of the

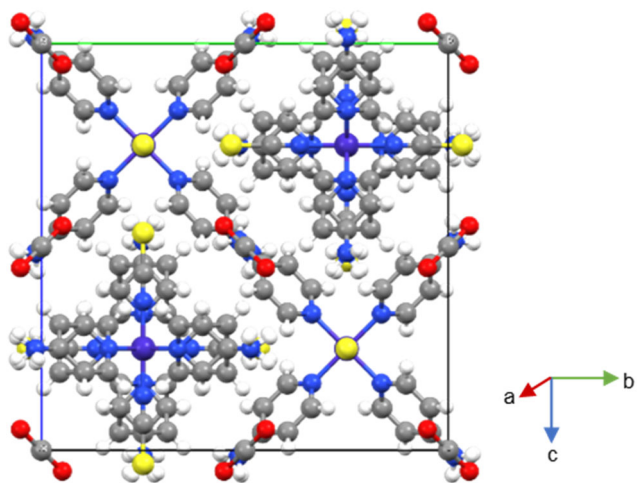


Fig 5. Crystal packing of the complex through a-axis

a, b, and c-axes indicates the high regularity of the arrangement of the $\text{Co}(4\text{-ampy})_4(\text{NCS})_2 \cdot \text{CO}_2$ complex.

The CO_2 molecules contained in the lattice occupy an advanced position on the cube and fill in between the intermolecular complex $[\text{Co}(4\text{-ampy})_4(\text{NCS})_2]$ as in Fig. 6. The C=O group of the CO_2 molecule also appears in the FTIR at 2398 cm^{-1} band. The O atom of the $[\text{Co}(4\text{-ampy})_4(\text{NCS})_2] \cdot \text{CO}_2$ molecule in one crystal lattice also forms an intermolecular hydrogen bond with the H atom of the amine group of the other aminopyridine molecule ($\text{C}=\text{O} \cdots \text{H}-\text{N}$). The intermolecular hydrogen bonds of ($\text{C}=\text{O} \cdots \text{H}-\text{N}$) that occur have two different lengths of 2.761 and 2.903 Å as shown in Fig. 6. The intermolecular hydrogen bonds of ($\text{C}=\text{O} \cdots \text{H}-\text{N}$) also appear on the Hirshfeld surface, where the $\text{O} \cdots \text{H}/\text{H} \cdots \text{O}$ intermolecular interaction contributes significantly to the Hirshfeld surface analysis (Fig. 6).

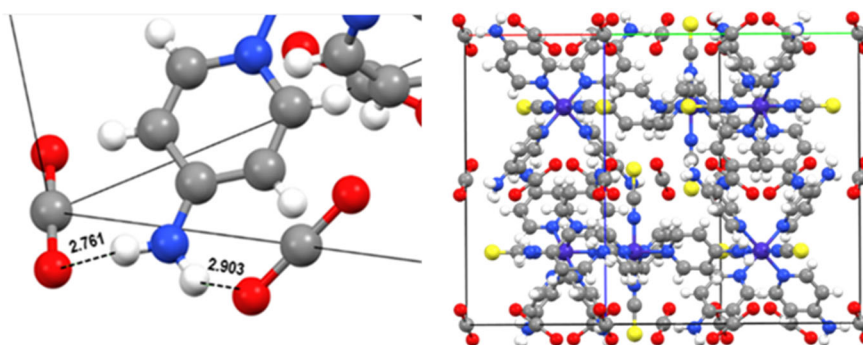


Fig 6. Interpretation of CO_2 position inside crystal lattice and intermolecular interaction

The four Co–N bond lengths of the pyridine ring of the 4-ampy ligand on the equatorial side have the same length of 1.982(3) Å. The two Co–N bonds of the isothiocyanate ligand at the axial position also have the same length of 1.903(4) Å. The size of the Co–N bond in the equatorial position is more extended when compared to the length of the Co–N bond from the axial position; this can be caused by the repulsion between the four 4-ampy ligands so that the distance caused becomes longer. The bond angle between the Co–N of the four N atoms of the pyridine ring and the two N atoms of isothiocyanates has the exact angle of 90° . The differences could be seen in $[\text{Co}(\text{SCN})_2(4\text{-}(\text{hydroxymethyl})\text{pyridine})_4]$ having Co–N bond angle in the range of $88.06(9)^\circ$ and $92.66(9)^\circ$ caused by the hydroxymethyl group which gave more steric effect than amino group in 4-ampy [13]. The bond lengths and angles, as shown in Table 3, indicate the geometry adopted by the structure of the $[\text{Co}(4\text{-ampy})_4(\text{NCS})_2] \cdot \text{CO}_2$ complex compound is octahedral, as shown in Fig. 7.

Hirshfeld Surface Analysis

Hirshfeld surface analysis and fingerprint plots were calculated to quantify the intermolecular interactions present in the crystal structure of the compound [27]. The normalized interaction distance (d_{norm}) description indicates the strength of intermolecular interactions [28–29]. The d_{norm} is calculated by the interaction distance of the nearest atom that is inside (d_i) to outside the surface (d_e) on a scale of -0.0249 (red) to 1.7498 (blue) [28].

Table 3. Bond length and bond angle of complex $[\text{Co}(4\text{-ampy})_4(\text{NCS})_2]\cdot\text{CO}_2$

Bond	Bond length (Å)	Bond angle	Angle (°)
Co-N3	1.903(4)	N3'-Co-N3	180.00
Co-N1	1.982(3)	N3-Co-N1	90.00
S1-C4	1.628(7)	N1-Co-N1'	90.00
N3-C4	1.132(7)	N3'-Co-N1'	90.00
N2-C3	1.341(6)	N3-Co-N1'	90.00
N1-C1	1.360(3)	N1-Co-N1'	90.00
C3-C2	1.400(3)	N1'-Co-N1'''	180.00
C2-C1	1.361(4)	N3'-Co-N1''	90.00
O1-C5	1.465(5)	N3-Co-N1''	90.00
-	-	N1-Co-N1''	180.00
-	-	N1''-Co-N1'''	90.00
-	-	N1'-Co-N1''	90.00
-	-	C4-N3-Co	180.00
-	-	C1-N1-C2'	115.90(3)
-	-	C2'-N1-Co	122.05(14)
-	-	C1-N1-Co	122.04(14)
-	-	N3-C4-S1	180.00
-	-	N2-C3-C2	121.91(17)
-	-	N2-C3-C1'	121.90(17)
-	-	C2-C3-C1'	116.20(3)
-	-	C1-C2-C3	120.40(2)
-	-	N1-C1-C2	123.50(2)
-	-	O1'-C5-O1	180.00(5)

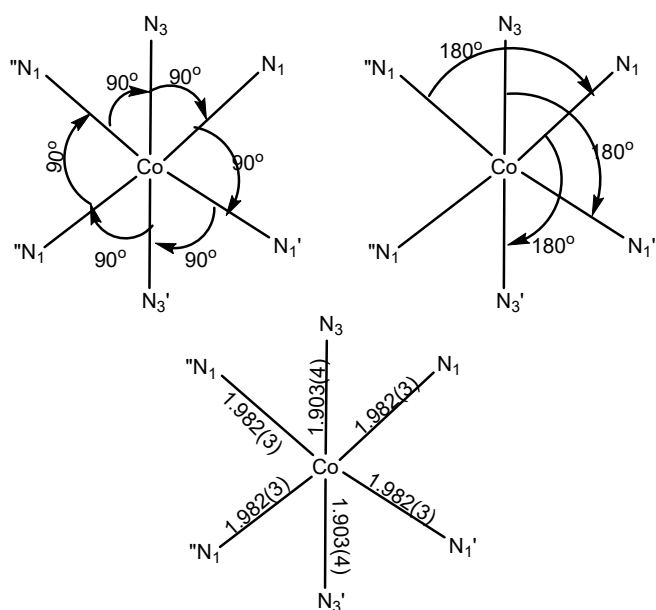
**Fig 7.** Bond length and bond angle of geometry complex $[\text{Co}(4\text{-ampy})_4(\text{NCS})_2]\cdot\text{CO}_2$

Fig. 8(a) shows red dots around the N and H atoms of the 4-ampy ligand, indicating intermolecular C-H interactions. Intermolecular interactions are weak in the blue and white areas. Fig. 8(b) shows a red area representing the presence of C-H- π interactions in the center of the pyridine ring. The blue region surrounding the red area offers the π - π exchange in the pyridine ring. Fig. 8(c) shows the curvature map and the flat surface represented by the blue and green areas [30]. The flat area around the pyridine ring indicates the presence of π - π interaction.

Fig. 9 shows the crystal fingerprint plot representing significant participation in intermolecular interactions on the Hirshfeld surface based on interatomic interactions and overall interactions [31]. The C \cdots H/H \cdots C interatomic interaction contributes the most to crystal stability, characterized by the most significant role on the Hirshfeld surface of 30.6%. The H \cdots H interaction has the second highest role with 24.3%, followed by the S \cdots H/H \cdots S interaction with 21.7%, and the O \cdots H/H \cdots O interaction with 14.5%. The O \cdots H/H \cdots O interaction comes from the intermolecular interaction between the H atom of the -NH₂ 4-ampy group and the O atom of the CO₂ molecule. Other minor interactions consist of S \cdots S, N \cdots H/H \cdots N, S \cdots O/O \cdots S, C \cdots C, and N \cdots O/O \cdots N at 5.3, 2.7, 0.4, 0.4, and 0.1%, respectively.

Antibacterial Activity

The antibacterial activity test was carried out on the synthesized compounds compared to reactants and solvents with positive control of chloramphenicol using the Kirby-Bauer agar diffusion method against *E. coli* (Gram-negative) and *S. aureus* (Gram-positive) bacteria [3,32-33]. The solvent used was 2% DMSO with a 2 mg/mL sample concentration. The tests were carried out using three repetitions (triplo) for each sample (Fig. 10) and the data in Table 4 is the average result of three inhibition zone diameter data.

The data generated is the diameter of the inhibition zone, which will be compared with the diameter of the positive control inhibition zone, namely chloramphenicol.

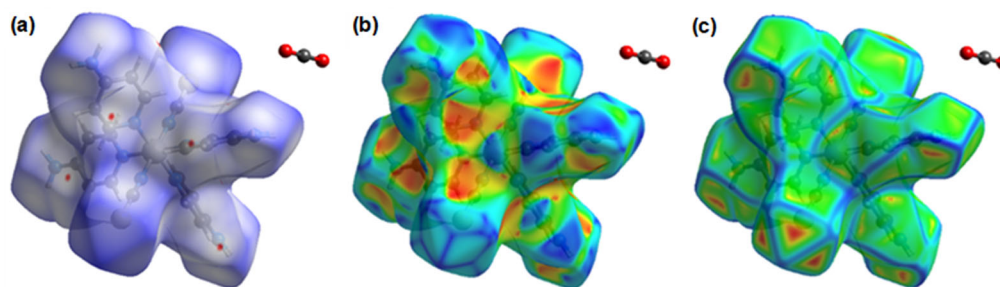


Fig 8. Hirshfeld surface analysis: (a) d_{norm} , (b) shape index, and (c) curvedness

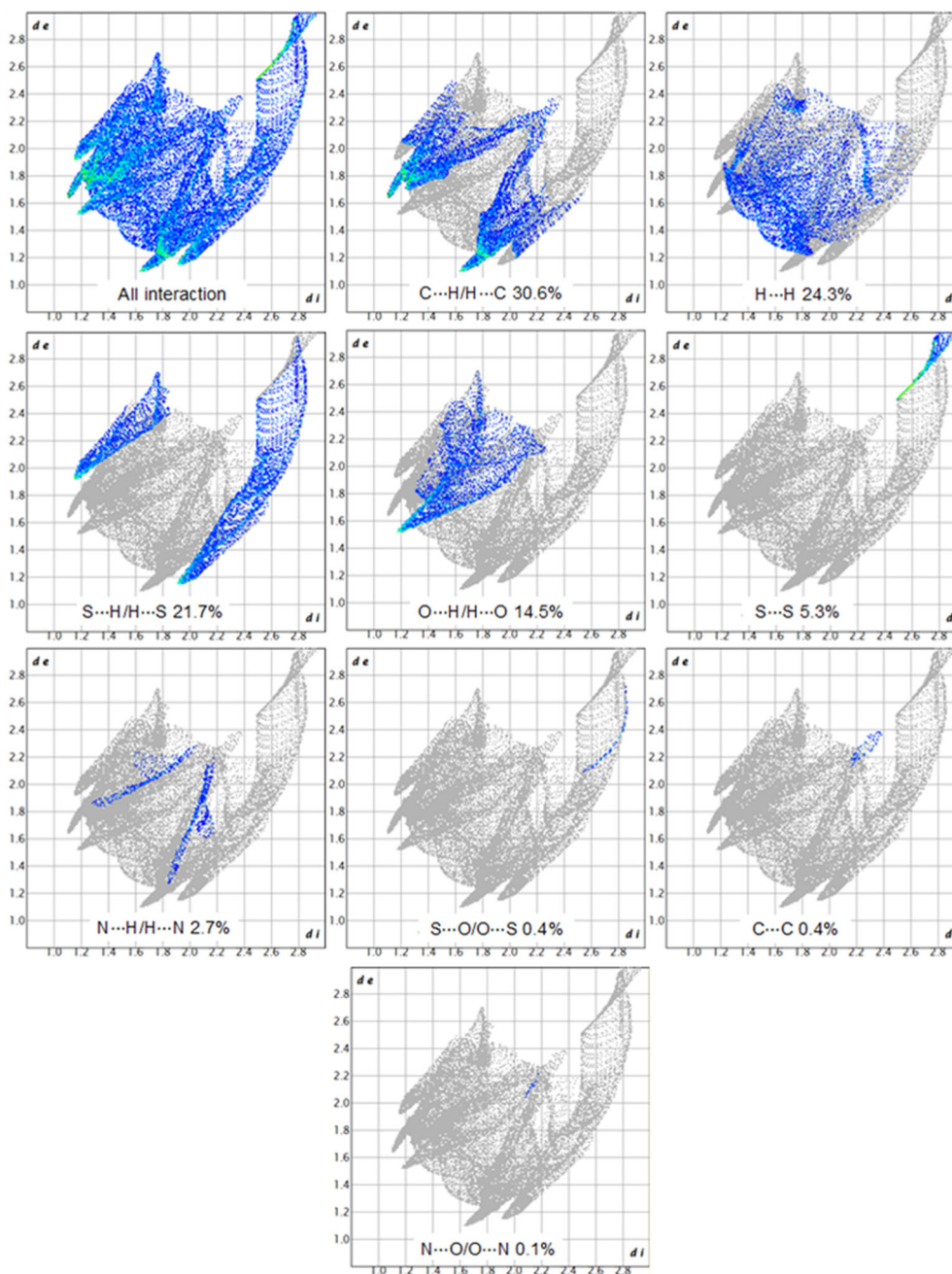


Fig 9. Fingerprint plot of complex $[\text{Co}(4\text{-ampy})_4(\text{NCS})_2] \cdot \text{CO}_2$

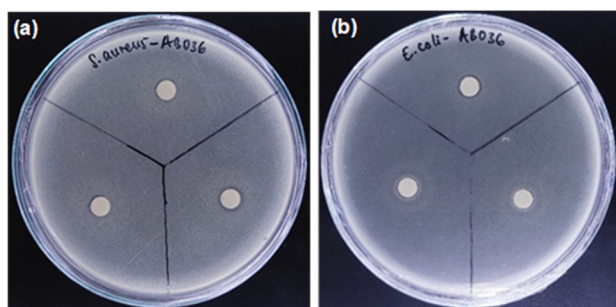


Fig 10. Inhibition zone of complex $[\text{Co}(4\text{-ampy})_4(\text{NCS})_2]\cdot\text{CO}_2$ against *S. aureus* dan *E. coli*

Table 4. Inhibition zone diameter of complex $[\text{Co}(4\text{-ampy})_4(\text{NCS})_2]\cdot\text{CO}_2$

Sample	Inhibition zone diameter	
	<i>S. aureus</i> (mm)	<i>E. coli</i> (mm)
As-synthesized complex	7.50	7.70
4-ampy	10.80	13.00
$\text{CoCl}_2\cdot 6\text{H}_2\text{O}$	17.00	11.20
KSCN	0.00	6.80
$\text{CoCl}_2\cdot 6\text{H}_2\text{O}$ + 4-ampy + KSCN	10.80	10.30
Chloramphenicol (+)	26.10	28.20

The synthesized complex produces much less spot area than chloramphenicol because there are more free electron pairs on chloramphenicol. This makes chloramphenicol more capable of making hydrogen bonds with bacteria. The inhibition zone diameter of the compound $[\text{Co}(4\text{-ampy})_4(\text{NCS})_2]\cdot\text{CO}_2$ on *S. aureus* was 7.50 mm smaller than that of *E. coli* at 7.80 mm. The equilibrium reaction between metal ions and their ligands can reduce the polarity of metal ions because their positive charge is shared with donor groups and delocalized [11,34-35]. Lipids and polysaccharides are essential cell walls and membrane constituents favorable for metal ion interactions. Reducing the polarity of these metal ions will increase the lipophilic character of the ligands. Consequently, the interaction between metal ions and lipids is favored, this can cause damage to the semipermeable cell barrier, disrupting bacterial cell processes [18,36].

Table 4 shows the compound $[\text{Co}(4\text{-ampy})_4(\text{NCS})_2]\cdot\text{CO}_2$ has less antibacterial activity than salt, ligand, and mixture, and this is because Gram-

negative bacteria have lipopolysaccharides in their cell walls that are non-polar. In contrast, Gram-positive bacteria have peptidoglycan, which is polar [37]. In the principle of like dissolve like, complexes with polar properties will easily penetrate thick peptidoglycan, and complexes that are non-polar will easily penetrate lipopolysaccharides [38-39]. The 4-ampy ligand has a pyridine ring, which is non-polar. As a result, the 4-ampy ligand showed an inhibition zone on Gram-negative bacteria of 13.00 mm and Gram-positive bacteria of 10.80 mm.

The antibacterial properties of the complex compound $[\text{Co}(4\text{-ampy})_4(\text{NCS})_2]\cdot\text{CO}_2$, when compared to the complex compound $[\text{Co}(2\text{-ampy})_2(\text{SCN})_2]$ [10], is still lower. Gram-positive bacteria such as *S. aureus* are more easily penetrated by more polar complex compounds as described, so the $[\text{Co}(2\text{-ampy})_2(\text{SCN})_2]$ complex compound with the 2-ampy ligand which is more polar than 4-ampy will be more accessible to penetrate the peptidoglycan wall. The antibacterial properties against Gram-negative bacteria themselves are difficult to compare because the $[\text{Co}(2\text{-ampy})_2(\text{SCN})_2]$ study used *S. typhi* bacteria, and this study used *E. coli* bacteria. The antibacterial properties of $[\text{Co}(4\text{-ampy})_4(\text{NCS})_2]\cdot\text{CO}_2$ synthesized with the antibacterial properties of $[\text{Co}(2\text{-ampy})_2(\text{SCN})_2]$ are difficult to compare precisely given the different test conditions, such as the solvent concentration used in this study is 2% DMSO. In comparison, in the study $[\text{Co}(2\text{-ampy})_2(\text{SCN})_2]$ used 10% DMSO solvent [10,40].

$\text{CoCl}_2\cdot 6\text{H}_2\text{O}$ salt has a very high solubility in the solvent, so it is effortless to penetrate the peptidoglycan in the cell wall of Gram-positive bacteria. This follows the results of the $\text{CoCl}_2\cdot 6\text{H}_2\text{O}$ salt antibacterial activity test, which shows the diameter of the inhibition zone on Gram-positive bacteria *S. aureus* by 17.00 mm and Gram-negative bacteria *E. coli* by 11.20 mm. KSCN has non-polar properties that easily penetrate lipopolysaccharides in Gram-positive bacteria, making it more effective for *S. aureus* (6.80 mm) than *E. coli* (0.00 mm).

The mixture of $\text{CoCl}_2\cdot 6\text{H}_2\text{O}$, 4-ampy, and KSCN compounds on Gram-negative and Gram-positive

bacteria is only effective in killing bacteria with an inhibition zone diameter of 10.30 and 10.70 mm, respectively. The mixture of $\text{CoCl}_2 \cdot 6\text{H}_2\text{O}$, 4-ampy, and KSCN compounds has better antibacterial activity because it works individually, each with different polarity properties.

■ CONCLUSION

The complex compound $[\text{Co}(4\text{-ampy})_4(\text{NCS})]_2 \cdot \text{CO}_2$ was successfully synthesized using the reflux method from the reaction between $\text{CoCl}_2 \cdot 6\text{H}_2\text{O}$, 4-ampy, and KSCN in methanol solvent. The synthesized compound is a purplish-red needle and cube-shaped crystal with octahedral geometry in a cubic lattice with space group $\text{P}\bar{1}3\text{n}$. The FTIR test revealed the presence of $\text{C}=\text{N}$ stretching vibration from NCS^- anion, $\text{C}-\text{N}$ vibration on amine group belonging to 4-aminopyridine ligand, and $\text{C}=\text{N}$ vibration of pyridine aromatic group. Hirshfeld surface analysis showed the highest contributing interactions in the complex were $\text{C}\cdots\text{H}/\text{H}\cdots\text{C}$, $\text{H}\cdots\text{H}$, $\text{S}\cdots\text{H}/\text{H}\cdots\text{S}$, and $\text{O}\cdots\text{H}/\text{H}\cdots\text{O}$. The antibacterial activity test of the synthesized complex was more active against *S. aureus* but less effective against *E. coli*.

■ ACKNOWLEDGMENTS

Many thanks delivered to Directorate General of Higher Education, Research, and Technology (Kemendibudristek of Indonesia) for Funding the DRTPM grant scheme PFR with contract number 20.6.44/UN32.20.1/LT/2023.

■ CONFLICT OF INTEREST

Authors declare no conflict of interest.

■ AUTHOR CONTRIBUTIONS

Linggar Agil Savitri and Faaza'izzahq Setta Putra conducted the experiment, collecting elementary data, graphing, and drafting. Sutandyo Dwija Laksmiana collected single crystal XRD data and structure refinement. Dewi Mariyam conducted data analysis, prepared manuscript draft, and organized the laboratories work. I Wayan Dasna conducted research designed, reviewed experiment procedures, reviewed and interpreted all data, wrote and revised manuscript, and manager of the project.

■ REFERENCES

- [1] Riaz, S., Zafar, W., Hassan, A.U., and Sumrra, S.H., 2021, Importance of coordination chemistry and role of sulfonamide derived compounds in biological activity – A review, *South. J. Res.*, 1 (1), 53–69.
- [2] Islam, F., Hossain, M.A., Shah, N.M., Barua, H.T., Kabir, M.A., Khan, M.J., and Mullick, R., 2015, Synthesis, characterization, and antimicrobial activity studies of Ni(II) complex with pyridine as a ligand, *J. Chem.*, 2015 (1), 525239.
- [3] Tsague Chimaine, F., Yufanyi, D.M., Colette Benedicta Yuoh, A., Eni, D.B., and Agwara, M.O., 2016, Synthesis, crystal structure, photoluminescent and antimicrobial properties of a thiocyanato-bridged copper(II) coordination polymer, *Cogent Chem.*, 2 (1), 1253905.
- [4] Yildiz, Y., 2017, "General Aspects of the Cobalt Chemistry" in *Cobalt*, IntechOpen, Rijeka, Croatia.
- [5] Paprocka, R., Wiese-Szadkowska, M., Janciauskiene, S., Kosmalski, T., Kulik, M., and Helmin-Basa, A., 2022, Lates developments in metal complexes as anticancer agents, *Coord. Chem. Rev.*, 452, 214307.
- [6] Turecka, K., Chylewska, A., Kawiak, A., and Waleron, K.F., 2018, Antifungal activity and mechanism of action of the Co(III) coordination complexes with diamine chelate ligands against reference and clinical strains of *Candida* spp., *Front. Microbiol.*, 9, 1594.
- [7] Abdulkareem, E.A., and Abdulsattar, J.O., 2022, Determination of nickel and cobalt in cosmetic products marketed in Iraq using spectrophotometric and microfluidic paper-based analytical device platform, *Baghdad Sci. J.*, 19 (6), 1286–1296.
- [8] Frei, A., Verdeosa, A.D. Elliott, A.G., Zuegg, J., and Blaskovich, M.A.T., 2023, Metals to combat antimicrobial resistance, *Nat. Rev. Chem.*, 7 (3), 202–224.
- [9] Amiri Rudbari, H., Iravani, M.R., Moazam, V., Askari, B., Khorshidifard, M., Habibi, N., and Bruno, G., 2016, Synthesis, characterization, X-ray crystal structures and antibacterial activities of Schiff base ligands derived from allylamine and their vanadium(IV), cobalt(III), nickel(II), copper(II),

- zinc(II) and palladium(II) complexes, *J. Mol. Struct.*, 1125, 113–120.
- [10] Munadhiroh, A., Wijaya, H.W., Farida, N., Golhen, S., and Dasna, I.W., 2022, Synthesis, characterization, and preliminary study of [Co(2-aminopyridine)₂(NCS)₂] or bis(2-aminopyridine)dithiocyanato cobalt(II) as an antibacterial, *J. Kim. Valensi*, 8 (1), 23–29.
- [11] Yuoh, A.C.B., Agwara, M.O., Yufanyi, D.M., Conde, M.A., Jagan, R., and Oben Eyong, K., 2015, Synthesis, crystal structure, and antimicrobial properties of a novel 1-D cobalt coordination polymer with dicyanamide and 2-aminopyridine, *Int. J. Inorg. Chem.*, 2015 (1), 106838.
- [12] Vamsikrishna, N., Kumar, M.P., Tejaswi, S., Rambabu, A., and Shivaraj, S., 2016, DNA binding, cleavage and antibacterial activity of mononuclear Cu(II), Ni(II), and Co(II) complexes derived from novel benzothiazole Schiff bases, *J. Fluoresc.*, 26 (4), 1317–1329.
- [13] Atakilt, A., Bayissa, G., Sendek, A., and Kibret, M., 2018, Cobalt(II) complexes with 1,10-phenanthroline alone and mixed with cytoside: Synthesis and antibacterial activities, *Ethiop. J. Sci. Technol.*, 11 (2), 79–96.
- [14] Jung, W.K., Koo, H.C., Kim, K.W., Shin, S., Kim, S.H., and Park, Y.H., 2008, Antibacterial activity and mechanism of action of the silver ion in *Staphylococcus aureus* and *Escherichia coli*, *Appl. Environ. Microbiol.*, 74 (7), 2171–2178.
- [15] Chandraleka, S., Ramya, K., Chandramohan, G., Dhanasekaran, D., Priyadharshini, A., and Panneerselvam, A., 2014, Antimicrobial mechanism of copper(II) 1,10-phenanthroline and 2,2'-bipyridyl complex on bacterial and fungal pathogens, *J. Saudi Chem. Soc.*, 18 (6), 953–962.
- [16] Rajalakshmi, S., Fathima, A., Rao, J.R., and Nair, B.U., 2014, Antibacterial activity of copper(II) complexes against *Staphylococcus aureus*, *RSC Adv.*, 4 (60), 32004–32012.
- [17] Hemeg, H.A., 2017, Nanomaterials for alternative antibacterial therapy, *Int. J. Nanomed.*, 12, 8211–8225.
- [18] Pasdar, H., Hedayati Saghavaz, B., Foroughifar, N., and Davallo, M., 2017, Synthesis, characterization and antibacterial activity of novel 1,3-diethyl-1,3-bis(4-nitrophenyl)urea and its metal(II) complexes, *Molecules*, 22 (12), 2125.
- [19] Mbani, A.L.O., Yufanyi, D.M., Tabong, C.D., Hubert, N.J., Yuoh, A.C.B., Paboudam, A.G., and Ondoh, A.M., 2022, Synthesis, crystal structure, DFT studies and Hirshfeld surface analysis of manganese(II) and cadmium(II) coordination polymers of 2-aminopyridine and dicyanamide, *J. Mol. Struct.*, 1261, 132956.
- [20] Dasna, I.W., Mariyam, D., Wijaya, H.W., Arrozi, U.S.F., and Sugiarto, S., 2023, Synthesis, structural determination and antibacterial properties of zinc(II) complexes containing 4-aminopyridine ligands, *Indones. J. Chem.*, 23 (4), 1108–1119.
- [21] Mariyam, D., Farida, N., Wijaya, H.W., and Dasna, I.W., 2022, Studi karakterisasi dan aktivitas antibakteri senyawa kompleks dari zinc(II) klorida, kalium tiosianat dan 2-aminopiridina, *J. Ris. Kim.*, 13 (1), 100–110.
- [22] Moore, M.H., Nassimbeni, L.R., and Niven, M.L., 1987, Studies in Werner Clathrates. Part 6. Structures of two novel polymeric inclusion compounds: Poly(bis(isothiocyanato)di(2-aminopyridine)nickel(II)-diethylether and di(aqua bis(isothiocyanato)3-aminopyridine μ -3-aminopyridine nickel(II))-water, *Inorg. Chim. Acta*, 132 (1), 61–66.
- [23] Laksamana, S.D., Wijaya, H.W., and Dasna, I.W., 2023, Synthesis, characterization, and antimicrobial of [Ni(2-ampy)2(dca)₂], *AIP Conf. Proc.*, 2634 (1), 020030.
- [24] Naghiyev, F.N., Khrustalev, V.N., Dobrokhotova, E.V., Akkurt, M., Khalilov, A.N., Bhattarai, A., Mamedov, İ.G., and Weil, M., 2022, Crystal structure and Hirshfeld surface analysis of 3-benzoyl-6-(1,3-dioxo-1-phenylbutan-2-yl)-2-hydroxy-2-methyl-4-phenylcyclohexane-1,1-dicarbonitrile, *Acta Crystallogr., Sect. E: Crystallogr. Commun.*, 78 (6), 568–573.

- [25] Spackman, P.R., Turner, M.J.T., McKinnon, J.J., Wolff, S.K., Grimwood, D.J., Jayatilaka, D., and Spackman, M.A., 2021, CrystalExplorer: A program for Hirshfeld surface analysis, visualization and quantitative analysis of molecular crystals, *J. Appl. Crystallogr.*, 54 (3), 1006–1011.
- [26] Svirchuk, Y.S., 2006, Electrical Conductivity, *A-to-Z Guide to Thermodynamics, Heat & Mass Transfer, and Fluids Engineering*, e (1), 1–13.
- [27] Al-Wahaibi, L.H., Joubert, J., Blacque, O., Al-Shaalan, N.H., and El-Emam, A.A., 2019, Crystal structure, Hirshfeld surface analysis and DFT studies of 5-(adamantan-1-yl)-3-[(4-chlorobenzyl)sulfanyl]-4-methyl-4H-1,2,4-triazole, a potential 11 β -HSD1 inhibitor, *Sci. Rep.*, 9 (1), 19745.
- [28] Babashkina, M.G., Panova, E.V., Alkhimova, L.E., and Safin, D.A., 2023, Salen: Insight into the crystal structure, Hirshfeld surface analysis, optical properties, DFT, and molecular docking studies, *Polycyclic Aromat. Compd.*, 43 (6), 5116–5138.
- [29] Barszcz, B., Masternak, J., and Kowalik, M., 2021, Structural insights into coordination polymers based on 6s² Pb(II) and Bi(III) centres connected *via* heteroaromatic carboxylate linkers and their potential applications, *Coord. Chem. Rev.*, 443, 213935.
- [30] Azouzi, K., Hamdi, B., Zouari, R., and Ben Salah, A., 2017, Synthesis, structure and Hirshfeld surface analysis, vibrational and DFT investigation of (4-pyridine carboxylic acid) tetrachlorocuprate(II) monohydrate, *Bull. Mater. Sci.*, 40 (2), 289–299.
- [31] Ben, O., Chebbi, H., and Faouzi, M., 2019, Synthesis, crystal structure, vibrational study, optical properties and Hirshfeld surface analysis of bis(2,6-diaminopyridinium) tetrachloridocobaltate(II) monohydrate, *J. Mol. Struct.*, 1180, 72–80.
- [32] Moustafa, I.M.I., Mohamed, N.M., and Ibrahim, S.M., 2022, Molecular modeling and antimicrobial screening studies on some 3-aminopyridine transition metal complexes, *Open J. Inorg. Chem.*, 12 (3), 39–56.
- [33] Raza, M.A., Kanwal, Z., Riaz, S., and Naseem, S., 2016, Antibacterial performance of chromium nanoparticles against *Escherichia coli*, and *Pseudomonas aeruginosa*, *The 2016 World Congress on Advances in Civil. Environmental and Materials Research (ACEM'16)*, Korea, August 28-September 1, 2016.
- [34] Claudel, M., Schwarte, J.V., and Fromm, K.M., 2020, New antimicrobial strategies based on metal complexes, *Chemistry*, 2 (4), 849–899.
- [35] Kędziora, A., Wieczorek, R., Speruda, M., Matolínová, I., Goszczyński, T.M., Litwin, I., Matolín, V., and Bugla-Płoskońska, G., 2021, Comparison of antibacterial mode of action of silver ions and silver nanoformulations with different physico-chemical properties: Experimental and computational studies, *Front. Microbiol.*, 12, 659614.
- [36] Sharma, B., Shukla, S., Rattan, R., Fatima, M., Goel, M., Bhat, M., Dutta, S., Ranjan, R.K., and Sharma, M., 2022, Antimicrobial agents based on metal complexes: Present situation and future prospects, *Int. J. Biomater.*, 2022 (1), 6819080.
- [37] Kleanthous, C., and Armitage, J.P., 2015, The bacterial cell envelope, *Philos. Trans. R. Soc., B*, 370 (1679), 20150019.
- [38] Zhuang, B., Ramanauskaite, G., Koa, Z.Y., and Wang, Z., 2021, Like dissolves like: A first-principles theory for predicting liquid miscibility and mixture dielectric constant, *Sci. Adv.*, 7 (7), eabe7275.
- [39] Mawardi, R.H., Sulistyani, N., Nurkhasanah, N., and Desyratnaputri, R., 2020, Antibacterial activity and TLC-bioautography analysis of the active fractions of *Muntingia calabura* L. leaves against *Staphylococcus aureus*, *J. Pharm. Sci. Community*, 17 (2), 69–75.
- [40] Sugiyama, H., Sekine, A., and Uekusa, H., 2015, Crystal structure of bis(4-aminopyridine)bis(isothiocyanato) cobalt(II), *X-Ray Struct. Anal. Online*, 31, 27–28.